Flooding as a sub-critical instability in open channels

Serge Mora, Martine Le Berre, Yves Pomeau

Flooding as a sub-critical instability in open channels

Serge Mora[1], Martine Le Berre[2] and Yves Pomeau[2]
[1] *LMGC, Université de Montpellier, CNRS, Montpellier, France*
[2] *LadHyX, École Polytechnique, Institut Polytechnique de Paris, Palaiseau, France*

In flood events caused by a gradual increase in the flow rate of a watercourse, the rise in water level is often abrupt, while the fall in level is delayed. We show that such behavior can be demonstrated by considering stationary flows at high Reynolds number in a prismatic open channel: several geometries of the channel cross-section lead to a subcritical instability that results in a discontinuous rise in the level when the flow rate exceeds a critical value F_i, and in a fall, also discontinuous, when the flow rate returns below a value F_o lower than F_i. This hysteretic behavior originates from the interplay between gravity which drives the flow downstream, and turbulent friction with the channel wall. The potential existence of several solutions arising from this bifurcation requires careful consideration in flood simulations.

I. INTRODUCTION

The issue of flooding is becoming increasingly problematic due to extreme events in a changing climate [1, 2], and it is still a challenge in fluid mechanics [3]. Despite the considerable progress that has been made in reducing the devastating effects of flooding, both in terms of prediction and preventive measures, a complete understanding of the physical phenomena involved in flooding is still incomplete. Recent developments are based on numerical models that can simulate watershed-scale flows from spatially-related data such as rainfall, land use and topography [4, 5], including situations involving several phases, for example with sediments in suspension [6, 7].

Flooding by river overflow is characterized by the quick invasion by water, typically overnight, followed by a much slower outflow [8]. Several factors have been identified in the literature to explain the contrast between flood and ebb times: (i) the low gradient with which accumulated water flows from extensive flooded areas towards the main watercourses or drainage systems [9], (ii) the low reabsorption of saturated soils or in areas where the soil is highly compacted [10], (iii) sediment deposits transported during flooding and settled on riverbanks and riverbeds as water levels fall, slowing down the drainage process [10].

Here we introduce an additional mechanism based on fluid mechanics to explain this behavior. We show that for uniform and stationary flows at high Reynolds numbers in prismatic channels of defined slope and cross-section, a sub-critical instability leads to an abrupt rise in level as flow increases in a quasi static manner, while the fall in level is delayed to lower flow rates. This scheme corresponds to a sub-critical bifurcation of the flow characterized by a hysteretic cycle so that within a range of flow rate, the water level is higher in the rising water phase than in the receding water phase. Hence, once the flood has occurred, the flooding persists until the flow rate falls back to a lower level than before the flood.

This article is organized as follows: Section II reviews why the average velocity of a stationary flow with a high Reynolds number and therefore turbulent in a prismatic channel depends, to a first approximation, on the cross-sectional area of the flow and the wetted perimeter via the ratio of these two quantities. In Section III, an instability condition relating to both the geometry of the prismatic channel and the flow law is derived. The consequences of this instability are analyzed for two generic types of straight channel section geometry (Sections IV and V), with evidence of hysteresis cycles. These cycles result in a discontinuous rise in the water level for a critical flow rate F_i when the latter is reached by increasing values, and a discontinuous decrease in the level for another critical flow rate F_o if the latter is reached downwards. Finally, the article ends with a discussion of the assumptions on which the theory is based, and the limitations they may entail.

II. UNIFORM AND STEADY FLOW IN PRISMATIC CHANNELS

For uniform, steady flow in prismatic open channels (whose properties are invariant in the direction of flow, see Section VI for a discussion of the limitations inherent in this assumption), various laws can be applied to express the mean flow velocity as a function of channel slope and dissipation. Chézy formula is still widely used in hydraulic engineering due to its simplicity and practical applicability in many real-life situations. Before the French Revolution, Chézy was given the task of bringing running water to Paris, a project going back to the beginning of the 17th century (and that only completted at the end of the 19th century). He derived his law by balancing input and friction. The input is the momentum given to water by gravity because water flows on an incline in the gravity field. The inclination angle between the surface of water and the horizontal plane will be denoted as i. For big rivers i is quite small, in the range of 1×10^{-2} rad or even less. The mass of water per unit length along the river is ρA where A is the cross-sectional area of the flow and ρ the mass density of water. The horizontal component of the pull of gravity on this mass

of water is (for i small)

$$\mathcal{F}_g = giA \tag{1}$$

Chézy assumed that friction occurs mainly at the bottom and sides of the river. Then, he estimated friction by extending Newton's recent quadratic law of drag of a blunt body at large velocities on friction to the banks of the river, stating that friction per unit length along the river is proportional to the wetted perimeter L of the cross-section (see Fig. 1), the mass density of the fluid and the square of the (average) velocity U,

$$\mathcal{F}_f = cLU^2 \tag{2}$$

with c the so-called "friction coefficient", or drag coefficient, depending on the Reynolds number and the roughness of the surface. Therefore the balance of forces yields [11]

$$U = \sqrt{\frac{gi}{c}\frac{A}{L}}, \tag{3}$$

In the literature, the Chézy formula is usually written as $U = C\sqrt{iA/L}$, where $C = \sqrt{g/c}$ is called the Chézy resistance coefficient. The Darcy-Weisbach law has the same formulation as Eq. 3, with the coefficient c no longer assumed to be constant. c in Eq. 3 is equal to one eighth of the Weisbach resistance coefficient [12]. Chézy measured the water input of small rivers near Paris, such as the Yvette and Bièvre running near Orsay and Bièvres to validate his law (Eq. 3) and he noticed that the drag coefficient (c) is higher in the summer when the weeds have grown than in winter. The drag coefficient, determined empirically for different types of surface, typically varies between 1×10^{-2} and 1×10^{-3} [13].

A friction force (per unit length) proportional to the wetted perimeter and the square of the velocity is supported by Prandtl boundary layer theory [14]. For example in pipes of circular cross-section the flow is assumed to be a plug flow (the velocity of the fluid is assumed to be constant except in the close vicinity of the boundary). The friction force along the pipe can be obtained by applying standard formulas for the pressure drop in turbulent pipe flows. Since all friction is in this boundary layer [15], this leads to a friction force per unit length equal to the perimeter of the pipe cross-section multiplied by ρU^2 times a drag coefficient c, with U the mean flow velocity [15]. The turbulent flow in a river or channel can also be approached, at high Reynolds number, by a plug flow in which the velocity gradients are localized near the walls and bottom of the river and the velocity is almost constant elsewhere and equal to U (Fig. 1) [14]. Therefore it is safe to assume that the friction at high Reynolds number is proportional to the length L of the wetted cross-section in water and the square of velocity U. For channels or rivers with rough or patterned bottom and walls, the wetted perimeter L to be considered must be obtained after spatial filtering of the actual profile, thereby excluding all asperities with characteristic dimensions lower than the boundary layer thickness. This filtering is straighforward for channel or river with straight cross-sections whose main dimensions are much larger than those of the asperities. Their effects are then taken into account through the coefficient of friction c.

In the frame of the mixing length model Prandtl derived an implicit relation linking the coefficient c to the Reynolds number Re named "Prandtl's universal law for smooth pipes". In the limit of a very large Reynolds number, it gives [14]:

$$c \propto \frac{1}{(\log(Re))^2}. \tag{4}$$

In the case of a plane Poiseuille flow, this relation was recently obtained with a different closure model based on an integral representation of Reynolds turbulent stress satisfying basic requirements of geometrical invariance, independently of any arbitrary length [16]. Eq. 4 was generalized for rough surfaces with empirical laws for friction coefficients showing that the Reynolds number dependence of c is even reduced by the surface roughness at high Reynolds number [17–20]. These laws have been successfully applied to free-surface flow in channels [12, 21].

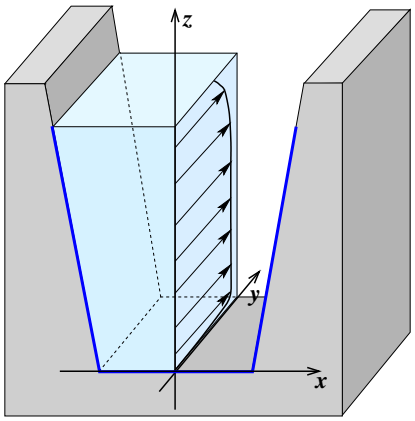

FIG. 1: Channel bed profile. The wetted perimeter of the cross-section, L, corresponds to the length of the blue lines. The x axis is horizontal and in the plane perpendicular to the main slope of the flow. The z axis points upwards. The velocity profile (black arrows) presented in the figure corresponds to a high Reynolds number flow.

In addition to the Chézy formula (Eq. 3), other empirically based formulas are used to model stationary, uniform, free-surface flows of water in channels. One of these, also widely used, is the Manning-Strickler formula,

$$U = 1/p\,(A/L)^{2/3}\,i^{1/2}. \tag{5}$$

p is the Manning coefficient, which is specific to the material and condition of the channel surface [22, 23]. Depending on the texture of the surfaces, it usually ranges

from $1 \times 10^{-2}\,\mathrm{m}^{-1/3}\,\mathrm{s}$ to $1 \times 10^{-1}\,\mathrm{m}^{-1/3}\,\mathrm{s}$. In what follows, we are dealing with flows with Reynolds numbers large enough that c in Eq. 3 or p in Eq. 5 can be regarded as a constant in a first approximation.

What is important here is that these laws lead, according to the arguments developed above to explain the physical origin of Chézy formula, to a velocity that is an increasing function of the A/L ratio:

$$U = f\left(A/L\right) \tag{6}$$

III. INSTABILITY CONDITION

In this section, we show that the relation between the flow rate F and the cross-sectional area of the flow A can be a non-monotonic function for specific channel cross-section geometries and flow rates. Such a decrease implies an instability, which is associated with a saddle-node bifurcation. At the bifurcation point, an infinitesimal increase in the flow rate leads to a finite increase in the cross-sectional area of the flow, a situation associated with flooding.

Assume that the banks are much flatter than the side walls of the river. As the level rises, the wet perimeter L increases and reaches more friction on a wider bottom. Therefore friction tends to decrease the flow speed so that, at a constant flow rate, it can be satisfied only by increasing the depth and so by reaching a higher A. This feedback describes the instability causing the flood. This depends on the particular shape of the channel, i.e. on the relation between L and A. To put this scheme into perspective, Eq. 6 is to be supplemented by a relation between the two parameters L and A as well as by the flow rate F that will be the control parameter. Fundamentally a flood is triggered by a slow change of F that increases first and then decay to return to its initial value. The control parameter F enters into the equation by the condition $F = UA$. Let us consider as variable quantity A. This maps the equation into a single one for A:

$$F = A.f(A/L) \tag{7}$$

This equation depends on the flow law f and the topography of the banks of the river through the function $L(A)$. There is a bifurcation in the solution if the derivative $\frac{dF}{dA}$ change its sign, from positive to negative, i.e. once (from Eq. 7):

$$f\left(\frac{A}{L}\right) < \frac{A^2}{L^2}\left(\frac{\mathrm{d}L}{\mathrm{d}A} - \frac{L}{A}\right) f'\left(\frac{A}{L}\right) \tag{8}$$

Since function f and its first derivative f' are positive, Eq. 8 is fulfilled for any bed profile in which $\mathrm{d}L/\mathrm{d}A$ can be far larger than L/A. Roughly speaking it says that if the length L changes fast enough as a function of the area A, then $\frac{\mathrm{d}F}{\mathrm{d}A} < 0$: an increase in L drives down the velocity U by friction and makes it impossible to keep the imposed flux. This generates multiple solutions in terms of A in Eq. 7.

In the particular case $U \propto (A/L)^n$, as for the Chézy formula ($n = 1/2$) or Manning formula ($n = 2/3$) the condition $\mathrm{d}F/\mathrm{d}A < 0$ simplifies to

$$\frac{\mathrm{d}L}{\mathrm{d}A} > \left(\frac{1+n}{n}\right)\frac{L}{A} \tag{9}$$

IV. RECTANGULAR DITCH SURMOUNTED BY A SLOPING BANK

In Section III, we have established the condition defining a bifurcation point in the $F - A$ parametric plane (Eq. 8). It depends on the geometry of the cross-section through $L(A)$ and the flow laws in the channels $f(A/L)$. For convex cross-sections (e.g. a U- or V-shaped profile), flow rate is always an increasing function of A: the steady height of water in the channel increases progressively and continuously as flow increases in a quasi-static way.

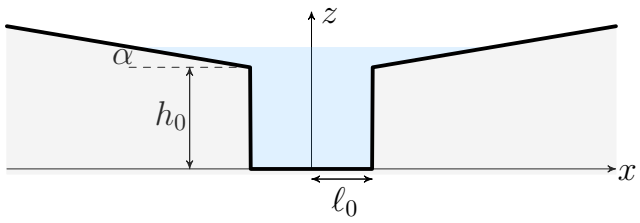

FIG. 2: Cross-section of a prismatic channel, composed of a rectangular ditch of height h_0 and width $2\ell_0$, surmounted by banks inclined at an angle α to the horizontal.

In this section, we consider prismatic channels with non-convex cross-sections consisting of a central rectangular ditch of width $2\ell_0$ and height h_0, surmounted on each side by an inclined plane with angle α to the horizontal acting as a floodplain, as depicted in Fig. 2. Let x be the horizontal axis in the direction perpendicular to the flow direction, and z the vertical axis. The wetted perimeter L and cross-sectional area A of the flow are:

$$\begin{aligned} L(z < h_0) &= 2\left(\ell_0 + z\right) \\ L(z \geq h_0) &= 2\left(\ell_0 + h_0 + \frac{z - h_0}{\sin(\alpha)}\right) \\ A(z < h_0) &= 2\ell_0 z \\ A(z \geq h_0) &= 2\ell_0 z + \frac{(z-h_0)^2}{\tan(\alpha)} \end{aligned} \tag{10}$$

The steady flow rate computed from Eq. 7 is plotted as a function of the cross-sectional area A in Fig. 3(a) with $h_0 = 2\ell_0$ and $\alpha = 0.05$, for both the Chézy and Manning formulas. The flow rate increases as a function of the cross-sectional area of the flow until it reaches a critical value, F_i (inflow). The flow rate then decreases as

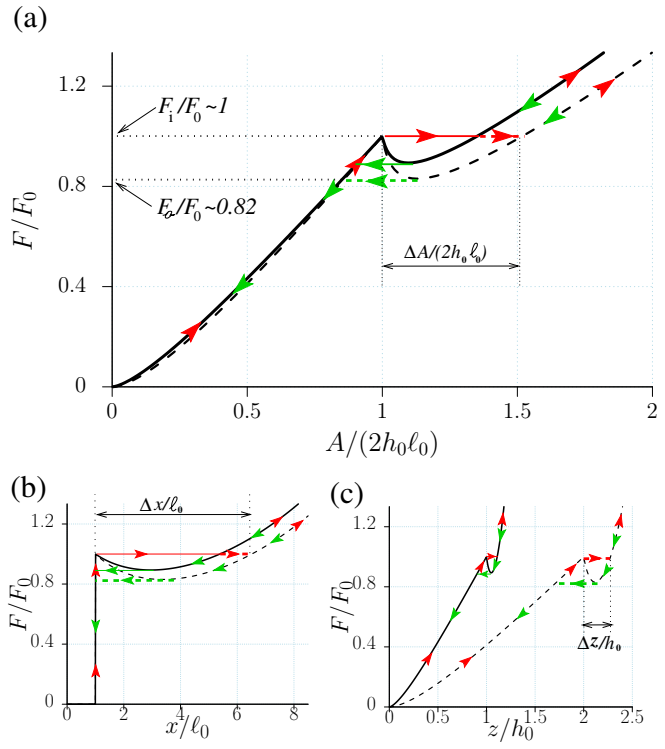

FIG. 3: Normalized flow rate F/F_0 calculated from Eq. 7 using the Chézy formula (solid lines, $n = 1/2$) or Manning formula (dotted lines, $n = 2/3$) for $h_0/\ell_0 = 2$. Flow rate F_0 is the flow rate calculated when the water head is exactly h_0. F/F_0 is plotted as a function of the cross-sectional area of the flow normalized by ditch area (a), as a function of water mirror width normalized by ditch width (b), and as a function of water head normalized by ditch depth (c). Red arrows indicate the direction of the path when the flow rate increases progressively, and green arrows indicate the direction of the path when it decreases progressively.

a function of the cross-sectional area of the flow until it reaches F_o (outflow). It then increases again. This non-monotonic behavior is associated with the occurrence of a saddle-node like bifurcation characterized by a hysteresis cycle in the cross-sectional area of the flow versus flow rate relationship. The red arrows in Fig. 3(a) depict the path in the $A - F$ plane during a quasi-static increase in flow, and the green arrows represent the path during outflow. The cross-sectional area of the flow increases in a non-continuous way when the flow crosses the F_i value. An infinitesimal increase in flow rate therefore has a dramatic effect on the the cross-sectional area of the flow. This situation is akin to flooding. The cross-sectional area of the flow also decreases abruptly when the flow crosses the F_o value downwards. Given that $F_i > F_o$, the sudden jump in the cross-sectional area of the flow during decay occurs at a lower flow rate than during the abrupt jump during flooding. In other words, for the same flow rate, the cross-sectional area of the flow is the largest during receding water levels. The growth and decay are not on the same branch of the hysteresis cycle. Thus the first stage (at increasing F) is much quicker because it happens with less friction on a narrower channel bottom, although the decay is longer because it happens on the upper branch where the flood is extended to larger and shallower river with more friction on the bottom.

Figures 3(b and c) represent the same hysteresis cycle as Fig. 3(a), in $x - F$ and $z - F$ parametric planes respectively. In the following, we refer to ΔA, $2\Delta x$, and Δz as the jumps in the cross-sectional area of the flow, in the water mirror width and the water height while the flow exceeds F_i (see Figs. 3(a-c)). Figs. 4(a-c) plot the variation of ΔA, Δx and Δz as a function of the angle α of the upper bank, for different values of the ratio h_0/ℓ_0, applying the Chézy and Manning formulas. In addition, Fig. 4(d) plots the gap between critical flow during inflow (F_i) and critical flow during outflow (F_o), normalized by the flow rate calculated when the water head is equal to the ditch depth. These gaps can take on significant values. For example, when $h_0 = \ell_0$, for $\alpha = 0.05$ and using the Manning formula, the cross-sectional area of the flow increases by more than 50% (Fig. 4(a)), the height then jumps by almost 20% (Fig. 4(b)) and the water bed width increases by more than 350% (Fig. 4(c)) as the flow overcomes the threshold value F_i. Still in this situation, flow F_i is around 25% greater than F_o (Fig. 4(d)). In addition, the curves in Fig. 4 show that the amplitudes of the ΔA, Δx and $F_i - F_o$ gaps associated with hysteresis are more pronounced with the use of the Manning formula than with the Chézy formula, and are more prominent the smaller the α angle. The existence of the maximum of Δz as a function of α is due to the fact that Δz is necessarily zero when $\alpha = 0$. We can also see from Figs. 4(a-d) that the hysteresis characteristics disappear beyond a certain angle α, which depends on the ratio h_0/ℓ_0. The ratio $\frac{dL/dA}{L/A}$ is at its maximum when $A = 2\ell_0 h_0$, just after the ditch is completely filled. The condition Eq. 9 evaluated for $A = 2\ell_0 h_0$ therefore provides the requirement for the instability to arise in the geometry considered here. This condition is $\alpha < \alpha_c$ with

$$\sin\alpha_c = \left(\frac{n}{n+1}\right)\left(\frac{1}{1+\ell_0/h_0}\right) \qquad (11)$$

In the limit $h_0 \gg \ell_0$ we obtain $\alpha_c = \arcsin\left(\frac{n}{n+1}\right)$, i.e. $\alpha_c \simeq 0.41\,\text{rad}$ (23.5°) using the Manning formula, and $\alpha_c \simeq 0.34\,\text{rad}$ (19.5°) using the Chézy formula. A steeper slope will never produce instability with this channel cross-section geometry, whatever the relative depth of the ditch.

V. CHANNELS WITH GRADUALLY FLARING BANKS

In section IV, channels with a central ditch were considered. The "reservoir" of the cross-sectional area of the

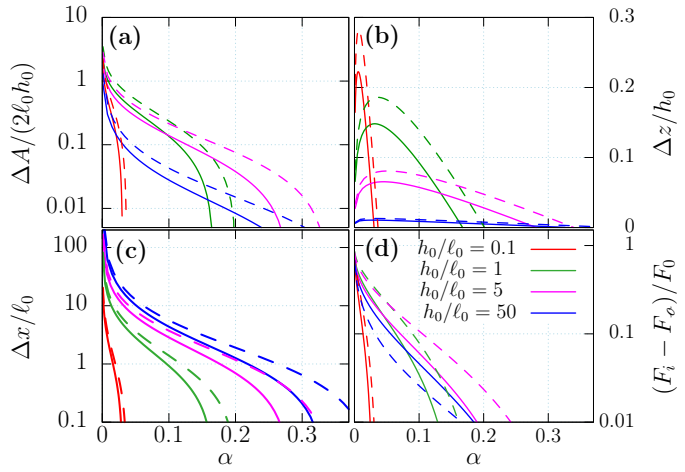

FIG. 4: Jump in cross-sectional area of the flow normalized by ditch cross-sectional area (a), jump in water head normalized by ditch height (b) and jump in water mirror width normalized by ditch width (c) as flow increases. Gap between critical flow during inflow (F_i) and critical flow during outflow (F_o), normalized by the flow calculated when the water head is equal to the ditch depth (d). The curves are calculated from Eq. 7 using the Chézy formula (solid lines, $n = 1/2$) or the Manning formula (dotted lines, $n = 2/3$). The ratios of h_0 to ℓ_0 are specified in the graphical legend in (d).

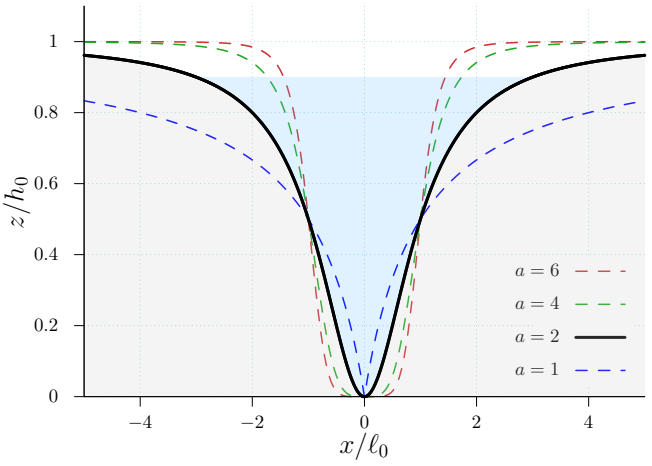

FIG. 5: Examples of channel cross-sections defined by $z(x) = h_0 \frac{(x/\ell_0)^a}{1+(x/\ell_0)^a}$ with $a = 1, 2, 4$ and 6.

flow formed by the poured ditch ($A = 2\ell_0 h_0$), combined with the low inclination of the newly covered banks, resulted in a wetted perimeter growth rate $\mathrm{d}L/L$ greater than the cross-sectional area growth rate of the flow, $\mathrm{d}A/A$, multiplied by $(1+n)/n$ (and thus the instability condition Eq. 9 was fulfilled). The slope (α) of the banks being constant, the ratio $\frac{\mathrm{d}L/\mathrm{d}A}{L/A}$ was unbounded and the instability condition Eq. 9 could only be verified on a limited portion of the section.

Let us now consider the example of a channel whose straight cross-section becomes more and more flared as we move away from its centerline. As an illustration, let us take straight cross-sections defined as:

$$z(x) = h_0 \frac{(x/\ell_0)^a}{1+(x/\ell_0)^a} \tag{12}$$

where h_0, ℓ_0 and the exponent a are constants. The variable x is the horizontal axis in the direction perpendicular to the flow direction, and z is the vertical axis (see Fig. 5). This choice of $z(x)$ does not claim to reproduce the precise geometry of channels. It does, however, highlight generic characteristic of cross-sections for which the instability described in Section III can occur.

The perimeter L and the area A as a function of the half-width of the bed x are computed as:

$$L(x) = 2\int_0^x \sqrt{1+(\mathrm{d}z/\mathrm{d}x)^2}\,\mathrm{d}x \tag{13}$$

$$A(x) = 2\left(xz(x) - \int_0^x z\,\mathrm{d}x\right) \tag{14}$$

Fig. 6 displays the flow rate calculated with Eqs. 7,13 and 14, for $h_0 = \ell_0$ and $a = 2$, plotted as a function of the half-width of the water mirror x. The flow rate, whether calculated using the Chézy or Manning formula, reaches a maximum (F_i) for a certain value of the width of the water mirror, and then declines as a function of x. In this case, the decrease in flow rate as a function of x continues as x tends towards infinity. Consequently,

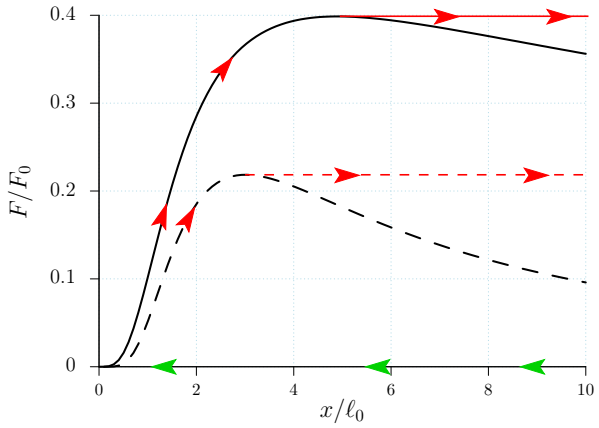

FIG. 6: Flow rate as a function of the half-width of the water mirror for a cross-section defined by $z(x) = h_0 \frac{(x/\ell_0)^2}{1+(x/\ell_0)^2}$ with $h_0 = \ell_0$, calculated from Eq. 7 using the Chézy formula (solid lines) or Manning formula (dotted lines). Red arrows indicate the direction of the path when the flow rate increases progressively, and green arrows indicate the direction of the path when it decreases progressively.

with an infinitesimal increase in flow at $F = F_i$, the flow switches from a stationary regime with a finite bed width to another stationary regime where the bed extension is infinite: the water has invaded the entire flood area.

Subsequently, a gradual reduction in flow rate will not succeed in resorbing this flooding, unless the flow rate returns to rigorously zero (see Fig. 6). The critical flow rate for outflow is, in these cases, $F_o = 0$.

In a real-world environment, a cross-section will not be represented correctly by Eq. 12 for values of x tending towards infinity, even with an added average roughness that takes account of asperities. However, it is enough for the topology to be roughly approximated up to the area of the riverbed capable of withstanding the flow rate F_o for a jump in width (or, equivalently, a jump in height) to occur. The values of the jump in height $h_0 - z_i$ when the

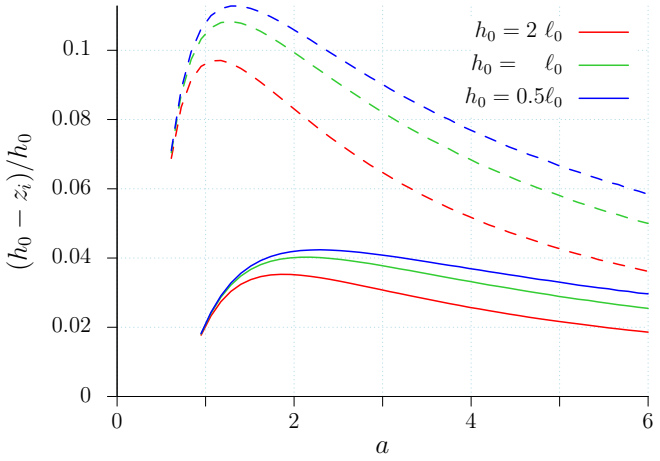

FIG. 7: Gap between channel height (h_0) and water head just before the jump ($z_i \to h_0$), normalized by channel height, as a function of parameter a, for $h_0/\ell_0 = 2, 1$ and $1/2$, calculated from Eq. 7 using the Chézy formula (solid lines) or Manning formula (dotted lines).

flow rate F_i is reached are plotted in Fig. 7 as a function of the exponent a for different values of the ratio h_0/ℓ_0. In the case of a cross-section as defined by Eq. 12 with $h_0 = \ell_0$ and $a = 2$, the flow rate F_i is reached when the water height z_i calculated using the Manning formula is equal to 90% of the maximum depth h_0. We have not determined the minimum value of exponent a for the instability to occur, but it appears that instability occurs even for values of a less than 1, for which the area of the cross-section of the channel is not bounded.

VI. CONCLUDING REMARKS

We have proposed a mathematical model based on the modeling of turbulent friction, leading to a sudden rise and a delayed recession of a river's course as a consequence of a sub-critical instability. The underlying physical mechanism has been highlighted on the basis of model situations, which consist of steady and uniform flow at a high Reynolds number, in channels with particular cross-sections. Modeling transient regimes would make it possible to estimate the times associated with the rise or fall of the water, which is an important issue that remains pending.

We have considered a prismatic channel, which rules out the existence of a hydraulic jump. A hydraulic jump is characterized by an abrupt transition from fast to slow flow (for example, in the vicinity of a channel slope change), often visible as a sudden rise in the water surface. The water then passes from a supercritical regime (fast and shallow) to a subcritical regime (slow and deeper) [24]. A sudden rise in river level following a slight increase in flow can then be observed. This situation is quite different from the one studied here, and should not be confused.

The instability we have considered here arises for certain shapes of channel cross-sections, whose profiles are non-convex. For these cross-sections, the relationship between the cross-sectional area of the flow and the permanent flow rate presents two discontinuities: (i) the first occurs when the flow reaches a critical flow rate F_i in increasing values, with an abrupt increase in the cross-sectional area of the flow, and (ii) a second discontinuity which occurs when a critical flow rate F_o is reached in decreasing values, with an abrupt decrease in the cross-sectional area of the flow. Since F_i is greater than F_o, the abrupt decrease occurs at a lower flow rate. The head-flow curve therefore exhibits hysteresis: backwater only occurs once the flow has declined substantially in comparison with the flow at which the rise in water level occurred.

The physical origin of this instability is well established: the increase in friction imposed by the geometry of certain cross-sections of channels when the water level rises leads to a reduction in the velocity of the flow. This reduction can be such that the flow rate is also reduced. With an imposed flow rate, a jump in the water level associated with hysteresis occurs. The particular shape of the governing flow law $f(A/L)$ (e.g. the Manning or Chézy formula) is not crucial: the main characteristics of the instability turn out to be robust with respect to this governing law. This fact gives us confidence that, even if the flow laws considered are only approximate laws of the real world, the conclusions drawn are robust enough to be transposed to situations closer to those encountered in the everyday environment. For example, in the case of a river with higher friction as the distance from the centerline increases (e.g. due to plant growth in areas usually closer to the water's surface), the reduction in velocity as the water level rises will be higher, making the effects of the instability all the more pronounced.

The occurrence of a sub-critical bifurcation leads to several possible solutions for the same set of conditions. This creates an issue for numerical simulations: it is necessary to ensure that these numerical models, which take into account complex elements such as details of topography, the presence of obstacles, suspended particles or temporal variations, can also lead to the

correct branch of solutions.

This instability occurs for turbulent flows at high Reynolds numbers, for which the velocity gradient in the cross-sections is negligible, except of course within the boundary layers [14]. In this case, because friction mainly occurs in the boundary layers, friction is approximately proportional to the wetted perimeter. This assumption is a limitation for the conditions of applicability of the theory. In addition to the Reynolds number being significantly greater than 1, we need to ensure that the boundary layer thickness, and therefore the wall and bottom roughness, is negligible compared to other characteristic lengths of the system (e.g. h_0 and ℓ_0). In this context, a turbulent flow modeling based on a local description would provide a quantitative determination of the limits of the plug flow hypothesis. In addition, numerical simulations should make it possible to establish the speed ranges for which the assumption of a high Reynolds number can be safely applied.

The possible implications are substantial, given the ever-increasing frequency and serious consequences of flooding. This work opens the way to strategies for mitigating flood amplitudes, for example by determining whether low-cost modifications to the bed profile or the characteristics of river walls could prevent the sudden rise in water levels that would follow the mechanism of this instability.

[1] N.W. Arnell and S.N. Gosling. The impacts of climate change on river flood risk at the global scale. *Climate Change*, 134:387–401, 2016.

[2] Intergovernmental Panel on Climate Change (IPCC). *Weather and Climate Extreme Events in a Changing Climate*, page 1513–1766. Cambridge University Press, 2023.

[3] P.D. Bates. Flood inundation prediction. *Annual Review of Fluid Mechanics*, 54:287–315, 2022.

[4] P.D. Bates and A.P.J. De Roo. A simple raster-based model for flood inundation simulation. *Journal of Hydrology*, 236:54–77, 2000.

[5] Tan M.L., P.W. Gassman, X. Yang, and J. Haywood. A review of swat applications, performance and future needs for simulation of hydro-climatic extremes. *Advances in Water Resources*, 143:103662, 2020.

[6] W. Wu. *Computational River Dynamics*. CRC Press, London, 2007.

[7] W. Wu and S.S. Wang. One-dimensional modeling of dam-break flow over movable beds. *Journal of Hydraulic Engineering*, 133:48–58, 2007.

[8] W.D. Shuster, Y. Zhang, A.H. Roy, F.B. Daniel, and M. Troyer. Characterizing storm hydrograph rise and fall dynamics with stream stage data. *Journal of the American Water Resources Association*, 44:1431–1440, 2008.

[9] S.X. Fan and S.W. Han. Testing research on the effects of land surface slopes upon surface runoff. *Bulletin of Soil and Water Conservation*, 11:6–10, 1991.

[10] H. Amit, V. Lyakkovsky, A. Katz, A. Starinsky, and A. Burg. Interpretation of spring recession curves. *Ground Water*, 40:543–551, 2002.

[11] A.D. Chézy. Mémoire sur la vitesse de l'eau conduite dans une rigole donnée. *MS Reprined in Annales des Ponts et Chaussées, Paris*, 60:1921, 1775.

[12] B.C. Yen. Open channel flow resistance. *Journal of hydraulic engineering*, 128:20–39, 2002.

[13] E.M. Shaw. *Hydrology in practice*. Stanley Thornes Ltd, Cheltenham, 1999.

[14] H. Schlichting, K. Gersten, H. Schlichting, and K. Gersten. *Fundamentals of boundary-layer theory. Boundary-layer theory*, chapter XX. Springer, 2000.

[15] L.D. Landau and E.M. Lifshitz. *FLuid Mechanics*. Pergamon Press, 1959.

[16] Y. Pomeau and M. Le Berre. Turbulent plane poiseuille flow. *The European Physical Journal Plus*, 136:1114, 2021.

[17] J. Nikuradse. Laws of flow in rough pipes. *National Advisory Committee for Aeronautics*, Technical Memorandum 1292:1–61, 1950.

[18] H.. Rouse. Critical analysis of open-channel flow resistance. *Journal of the Hydraulic Division*, 91:1–23, 1965.

[19] C.F. Colebrook. Turbulent flow in pipes, with particular reference to the transition region between the smooth and rough pipe laws. *Journal of the Institution of Civil Engineers*, 11:133–156, 1938.

[20] B.J. McKeon, M.V. Zagarola, and A.J. Smits. A new friction factor relationship for fully developed pipe flow. *J. Fluid. Mech.*, 538:429–433, 2005.

[21] L.F. Moody. Friction factors for pipe flow. *Transactions of the ASME*, 66:671–684, 1944.

[22] R. Manning. On the flow of water in open channels and pipes. *Transactions Institute of Civil Engineers of Ireland*, 20:161–209, 1895.

[23] J.C.I. Dooge. The manning formula in context, in channel flow resistance: Centennial of manning's formula. *Water Ressources Publications*, 1992.

[24] H. Chanson. Current knowledge in hydraulic jumps and related phenomena. a survey of experimental results. *European Journal of Mechanics - B/Fluids*, 28:191–210, 2009.